00ICES-141

Fabrication of laterally coupled InGaAsSb-GaSb-AlGaAsSb DFB laser structures

Y. K. Sin, R.N. Bicknell-Tassius, R. E. Muller, S. Forouhar
Jet Propulsion Laboratory, California Institute of Technology

Randy D. May
SpectraSensors, Inc., Altadema CA,

ABSTRACT

The development of tunable diode laser systems in the 2 – 5 μm spectral region will have numerous applications for trace gas detection. To date, the development of such systems has been hampered by the difficulties of epitaxial growth, and device processing in the case of the Sb-based materials system. One of the compounding factors in this materials system is the use of aluminum containing compounds in the laser diode cladding layers. This makes the regrowth steps used in traditional lasers very difficult. As an alternative approach we are developing laterally coupled antimonide based lasers structures that do not require the regrowth steps. In this paper, the materials growth, device processing and development of the necessary drive electronics for an antimony based tunable diode laser system are discussed.

INTRODUCTION

Future long duration manned space missions will require the monitoring of toxic and volatile gases of enclosed spaces. Tunable diode laser (TDL) spectroscopy provides a means in which trace gases can be accurately monitored using systems that are relatively small in size and low in power consumption.

Two basic techniques are routinely employed for laser control and signal processing using tunable diode lasers: scanning and line-locking. In a scanning TDL spectrometer the laser wavelength is repetitively swept across a small wavelength interval to record full spectrum lineshapes which are then analyzed to determine the gas concentration. Various modulation and detection schemes have been developed to increase signal-to-noise ratio (SNR), the simplest of which is wavelength modulation by modulation of the laser injection current. Demodulation at some multiple of the modulation frequency produces harmonic lineshapes which are a function of the molecular lineshape, the modulation amplitude, and the modulation waveform. Higher frequency (MHz to GHz) modulation schemes have also been implemented which obtain shot noise limited sensitivities in the laboratory. However, optical interference fringes in the spectra generally limit the SNR that can be obtained with a field instrument, and these effects are usually considerably larger than any other noise source in the spectra. Higher frequency modulation techniques are also more difficult to implement experimentally, and the spectral lineshapes can be complicated. Choosing the optimum modulation and detection frequencies for a scanning TDL field spectrometer is a tradeoff between experimental simplicity and ultimate potential SNR.

In a line-locked spectrometer the laser wavelength is held fixed at the exact center of a spectral line (or a fringe peak from an etalon) using an active servo loop. Various experimental implementations are possible, but the most common is to use a first or third derivative spectrum which has a zero crossing at the spectral line center. By fixing the laser wavelength at line center, direct or differential gas concentration measurements can be made by simple application of the Beer Lambert Law. Experimentally, a line-locking spectrometer requires a beamsplitter, a reference gas cell or stabilized etalon, and a second detector for implementation of the line-locking servo loop. Thus, component costs are higher than for a simple wavelength modulation sensor. Because the laser wavelength is held fixed and the basic measurement consists of monitoring a DC signal level, system response time can be extremely fast (ms). However, methods must be incorporated to account for the various sources of drift in a line-locking system, and these generally require interrupting the measurement to acquire zero and span calibrations. In principle, a scanning spectrometer with proper laser control

waveform eliminates the need for such calibrations. In practice confirmation of the sensor calibration must be performed on a regular basis for any critical applicaion, but the frequency of these checks can be much less that for a line-locking system thus reducing consumable costs and maintenance costs.

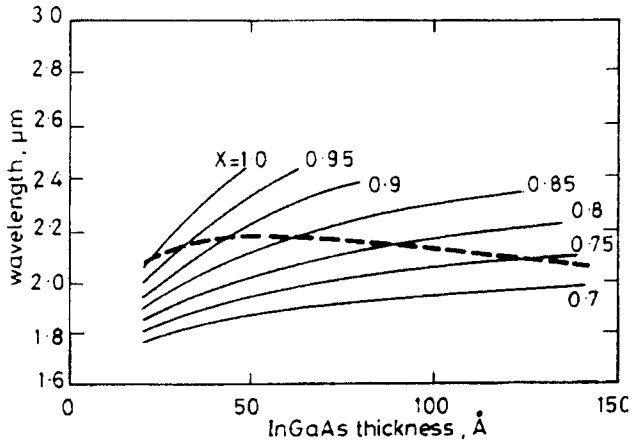

Figure 1: *Calculation of wavelength against thickness for compressively strained $In_xGa_{1-x}As$ compositions for x=0.7 to 1.0. - ----- limit on critical thickness for strained layer*

Many simple molecules have strong absorption band in the wavelength region between 1.0 and 5.0 μm. These include H_2O, CO_2, CO, and N_2O and others. The mature technology of near-IR 1.3 and 1.55 μm InGaAsP/InP diode lasers for fiberoptic communication has been extended to fabricate lasers that emit anywhere in the wavelength range of 1.1- 1.7 μm. Compressively strained InGaAs quantum well structures on InP substrates have been used for the development of semiconductor lasers operating beyond 1.65 μm. We have previously reported the room temperature operation of InGaAs/InP quantum well lasers at wavelengths as long as 2.06 μm[1,2]. In general, the InGaAs material wavelength increases with increased In composition and decreases under compressive strain and due to quantum size effects. The wavelength of the fundamental transition of strained InGaAs quantum well can be calculated using a finite square well potential. The calculated bandgap wavelength as a function of quantum well thickness at T=300°K, is shown in Figure 1. The dashed line in this figure shows the maximum bandgap wavelength achievable with various In compositions without exceeding the critical thickness which was calculated on the basis of the force balance model proposed by Mathews and Blakeslee [3]. This calculation shows that the strained InGaAs quantum well on InP substrates is fundamentally limited to emission wavelengths shorted than about 2.1 μm. Semiconductor lasers with emission wavelengths longer than 2.0 μm are of a great interest due to there ability to access the fundamental absorption bands of many molecules rather than overtones. Tunable diode laser absorption spectrometers operating in the wavelength region of the fundamental absorption would have sensitivities that greatly exceed those relying on overtone absorption.

Antimony based lasers have attracted a great deal of attention as alternatives to InP-based lasers due to the fact that their fundamental energy gaps lie in the 2.0μm – 5μm wavelength region, thus extending the accessible wavelength region for TDL's. High performance antimony based lasers have been reported including ultra-low threshold current density [4], high power operations [5], and operation at temperatures up to 130°C[6]. Even though single longitudinal mode lasers such as distributed feedback (DFB) or distributed Bragg reflector (DBR) lasers are highly desirable for these lasers to be effectively applied to chemical sensing applications, there have been very limited reports of single mode antimonide-based lasers [7]. DFB lasers achieve wavelength selectivity though feedback from a periodic change in index or gain along the cavity. This usually requires an interrupted growth, i.e. regrowth over a grating structure, in the fabrication process which greatly increases the potential of the introduction of defects at the grating/regrowth interface. Determining the proper surface preparation and growth parameters to achieve high quality epitaxial regrowth while preserving the grating structure is technically demanding, particularly with antimony based laser structures in which oxidation is problematic due to the use of AlGaAsSb in the cladding layers. One way to eliminate the regrowth problem is to etch the gratings after the lasing cavity has been fabricated and rely on the coupling of the evanescent electromagnetic fields. This has been demonstrated by etching the gratings directly above the waveguide and injecting the current from the side or by etching the gratings through the cap and upper cladding layer to provide the index guiding for the ridge and selective feedback[8,9]. An alternative approach is to etch the ridge first and then define the gratings on both sides of the ridge. This approach has been recently reported on LC-DFB ridge waveguide lasers in the InGaAs-GaAs-AlGaAs material system with excellent d.c. and spectral characteristics [10,11] and is shown schematically in Figure 2.

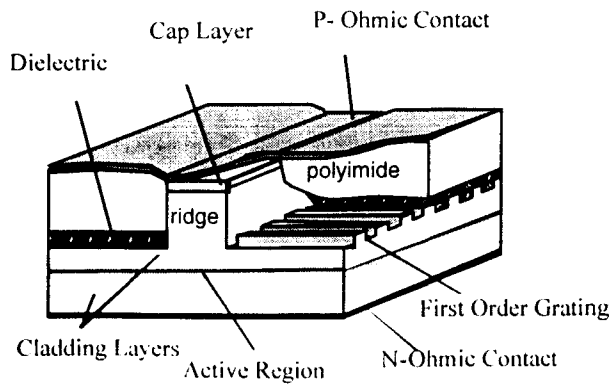

Figure 2: *Schematic diagram of a laterally-coupled DFB laser*

In this paper, we report on the crystal growth and the fabrication of InGaAsSb-GaSb-AlGaAsSb laterally-coupled ridge waveguide distributed feedback laser structures, along with the development of control electronics and packaging of a trace gas sensor based on InGaAsSb laser diodes.

Figure 3: *SEM cross-section of first order gratings formed in AlGaAsSb layer on GaSb substrate*

Experimental Methods

MBE Growth of Antimony Based Laser Structures

Molecular beam epitaxy (MBE) was employed for the growth of all the epitaxial layers and laser structures reported here. Te-doped GaSb (100) substrates were employed. The substrates were briefly etched in concentrated HCl and then rinsed in isopropanol, blown dry and then mounted and loaded into the Riber MBE32P MBE system. Calibration and small test structures were indium mounted. To avoid stresses during thermal cycling, larger samples and laser structures were grown using indiumless mounting sample holders. The MBE system was equipped with In, Ga, Al, and two antimony standard effusion cells. An arsenic valved cracker was employed to provide a precisely controllable flux of As_4. N- and p-type dopant were GaTe and Be, respectively. These provided p-type carrier concentrations up to $2x10^{18}$ cm^{-3} in GaSb and up to $1x10^{18}$ cm^{-3} in the aluminum containing compounds. N-type concentrations up to $1x10^{17}$ cm^{-3} were routinely obtained in AlGaAsSb and $1x10^{18}$ cm^{-3} in GaSb epitaxial layers.

Substrates were heated under an Sb_4 flux to desorb the surface oxides. Upon oxide desorption the samples showed a strong (3x1) surface reconstruction, indicative of an atomically smooth clean surface. This desorption temperature along with the (3x1) to (5x1) surface reconstruction transition temperature were used to accurately determine the substrate temperatures employed. In the present work, aluminum containing layers were grown in the range of 490-510 °C, while the other layers were grown in the range of 430-480 °C. Growth temperatures and V/III ratios were optimized to grow laser structures with high optical and structural qualities.

The laser structures had multiple quantum well (MQW) active layers consisting of either InGaAsSb quantum well/AlGaAsSb barrier (Type I) or InGaAsSb quantum well/GaSb barrier (Type II) that were sandwiched between AlGaAsSb cladding layers. Finally, p-doped GaSb layers were grown as contact layers.

Reactive Ion Etching (RIE) and Grating Formation

All etching experiments were performed in a parallel-plate etching system operating at 13.56 MHz. The samples were placed on a quartz plate with a diameter of 30cm that covered the capacitively coupled rf-driven electrode, and the gases were introduced through holes in the upper electrode. The electrodes were water cooled, and the system was pumped by a turbo molecular pump to a base pressure of $\sim 3x10^{-7}$ Torr. Electron-beam writing was chosen over holography for grating fabrication due to the flexibility of e-beam writing. With this technique multiple pitch gratings can be written on a single wafer to allow precise matching of the laser emission wavelength to the desired absorption band.

Experimental Results

Ridge Waveguide Formation by RIE

Ridge waveguides were formed in an AlGaAsSb upper cladding layer of the laser structure grown on n-GaSb substrate as follows. First, a 120nm thick oxide film was deposited by plasma enhanced chemical vapor deposition (PECVD) at 250°C, and patterned by standard photolithography to form ~5μm wide stripes. Reactive ion etching using a mixture of CF_4 and O_2 gases was employed to etch the oxide film. The photoresist was then removed and the wafer was loaded into a second RIE chamber where a mixture of BCl_3 (14 sccm) and Ar (1 sccm) was used to form ~1.5μm high ridges. The total process pressure for the ridge etching was 10 mtorr, the rf power density was $0.2W/cm^2$, and the d.c. bias was -520V.

Smooth side walls were obtained as evidenced by SEM cross-section of the ridge waveguide formed in AlGaAsSb layer, and the etching rate was 110nm/min.

Grating Fabrication by RIE

First order gratings were fabricated in GaSb substrates as well as in AlGaAsSb upper cladding layers.

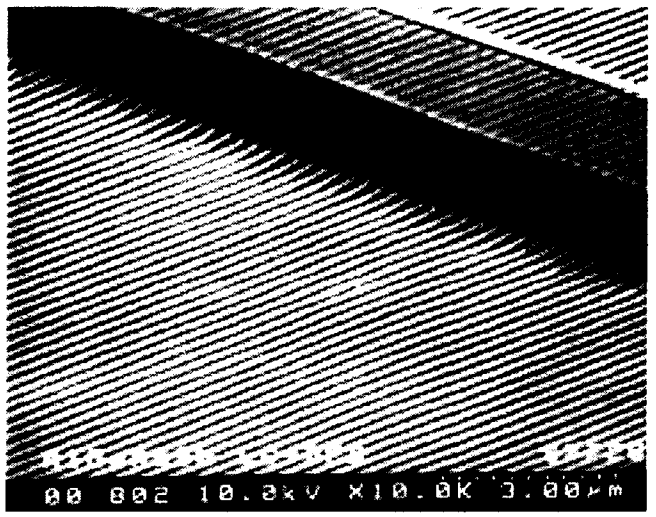

Figure 4: *SEM image of an AlGaAsSb LC-DFB laser structure*

Polymethyl methacrylate (PMMA) 0.2µm thick was deposited on the samples by spin-coating, and then a 50keV JEOL electron-beam exposure system was used to write ~20µm wide lines for first order gratings (the corrugation pitch was ~300nm). Electron-beam doses were optimized to obtain a grating duty cycle of ~50% in PMMA. After developing, samples were introduced in to the RIE chamber.

For GaSb etched gratings, only BCl_3(7sccm) was used with the total process pressure of 10mtorr and the rf power density of 0.2W/cm^2. Square-shaped gratings were obtained with smooth surfaces and sidewalls as well as with high uniformity. The etching rate was 2.0nm/sec, and a duty cycle of ~50% was obtained.

Gratings were also formed in AlGaAsSb using the same process conditions as for gratings in GaSb. As shown in Figure 3, very uniform square-shaped grating patterns were obtained with a duty cycle of around 50%. The etching rate was 16.5Å/sec.

To the best of our knowledge, this is the first demonstration of grating fabrication in the GaSb-based material system in which high quality and controlled grating shapes have been obtained.

Laterally-coupled DFB Laser Structures

The following processing steps were used to fabricate laterally-coupled DFB laser structures. Silicon dioxide, 120nm-thick, was deposited by PECVD, followed by standard photolithography and RIE using CF_4 and O_2 to define 4µm-wide oxide stripes. Reactive ion etching was then employed to form 1.5µm high ridges using BCl_3 and Ar. This procedure resulted in smooth surface and sidewall morphology.

The sample was then spin coated with PMMA and the e-beam exposure system was used to write 20µm wide lines for first order gratings along the ridge. Gratings were formed in AlGaAsSb cladding layer by RIE using only BCl_3. Uniform grating patterns were obtained. Excellent controllability of the grating heights and duty cycle was also demonstrated. In Figure 4 is shown a SEM image of an antimony based LC-DFB laser structure. A SEM cross-section of first order gratings formed in the upper AlGaAsSb cladding layer of the laser structure after staining is shown in Figure 5.

Work is presently being focused on LC-DFB lasers with the emission wavelengths near 2.3µm, and the lasing characteristics of these lasers will be reported elsewhere.

Sensor Electronics and Packaging

There are many applications where rapid monitoring of gases using a portable sensor is desired. Cost, power consumption, and physical size have been major obstacles to the widespread use of TDL-based gas sensors for such applications. The lack of availability of lasers at a reasonable cost has also prevented development of a portable TDL sensor. We have incorporated the control electronics, laser diode and detector into a hand-held, battery operated humidity

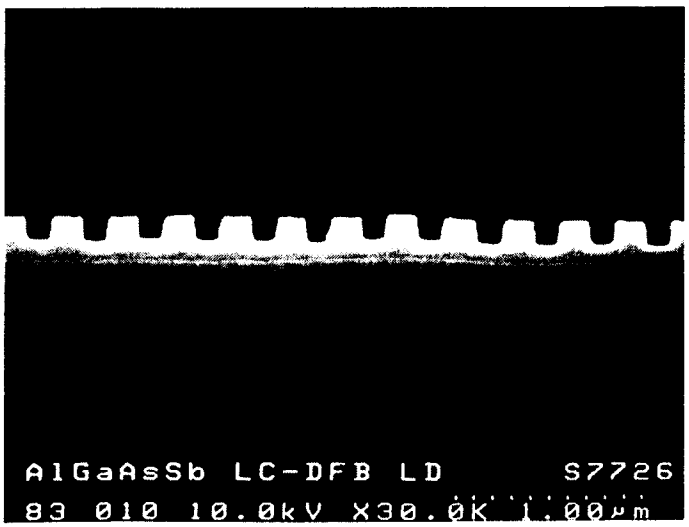

Figure 5: *SEM cross-section of gratings formed in AlGaAsSb clad layer of LC-DFB laser structure (also visible is the active layer under the gratings).*

sensor that is diagrammed in Fig. 6. A coarse screen surrounds the optical head to ensure adequate flow of

Figure 6: *Diagram of a hand-held TDL sensor which has been designed and constructed for multiple applications. Dimensions are 8.9 x 17.8 x 4.4 cm, +5V or battery operated, real-time display*

air across the sample region. A modified version of this sensor contains a small multi-pass Herriot cell attached to the long side of the enclosure for measurements of other trace gases. The control electronics are identical to the humidity sensor and the data processing matrix for the specific gases are stored in an on-board one-time programmable EPROM. The system is designed so that any operational parameters or data processing information that differs from one sensor to another (e.g. different target gases, different optical configurations, etc.) can be stored in the EPROM and updated as necessary (by replacement of the EPROM).

Battery life in such a sensor system depends on the laser operating temperature relative to the ambient since the primary source of power draw is the thermoelectric cooler (TEC) which controls the laser operating temperature. By developing lasers which operate at temperatures above +30°C, the TEC works primarily as a heater which is much more efficient than cooling. Three AA sized batteries provide approximately three hours of operation. A belt-worn battery pack can provide up to 12 hours of operation. Operation from a single +5V supply is also possible, and the main system enclosure contains an internal recharging circuit that recognizes the presence of an external 5V supply. When powered from an external supply the batteries are recharged while the system operates from the supply. So the system can be removed from the external supply and carried to another location without having to be powered down and restarted.

CONCLUSION

In conclusion, we have grown high quality InGaAsSb-GaSb-AlGaAsSb strained MQW laser structures by MBE, and also developed, for the first time, dry etching processes that are suitable for antimony based laterally coupled DFB lasers. Finally, drive electronics and packaging techniques have been developed and constructed for a hand held tunable diode laser system employing laser diodes based on InGaAsSb.

ACKNOWLEDGMENTS

Part of the work described in this paper was performed by the Center for Space Microelectronics Technology, Jet Propulsion Laboratory, California Institute of Technology under contract with the National Aeronautics and Space Administration

REFERENCES

1. S. Forouhar, S. Keo, A. Larsson, A. Ksendzov, and H. Temkin, Electron. Lett. 29 , 574(1993).
2. S. Forouhar, A. Ksendzov, A. Larsson, and H. Temkin, Electron. Lett. 28, 1431(1992).
3. J.W. Mathews, and A. E. Blakeslee, J. Cryst. Growth, 27, 118 (1974).
4. G. W. Turner, H. K. Choi, and M. J. Mantra, Appl. Phys. Lett. 72, 876 (1998)
5. H. K. Choi, J. N. Walpole, G. W. Turner, M. K. Connors, L. J. Missaggia, and M. J. Manfra, IEEE Photon. Technol. Lett. 10, 938 (1998).
6. D. A. Yarekha, G. Glastre, A. Perona, Y. Rouillard, F. Gentry, E. M. Skouri, G. Boissier, P. Grech, A. Joullie, C. Alibert, A.N. Baranov, Electron. Lett. **36**, 537(2000)
7. T. Bleuel, M. Brockhaus, J. Koeth, J. Hofmann, R. Werner, and A. Forchel, SPIE (1999)
8. Z. L. Liau, D. C. Flanders, J. N. Walpole, N. L. Demeo, Appl. Phys. Lett. **46**, 221(1985).
9. L. M. Miller, J. T. Verdeyen, J. J. Coleman, R. P. Bryan, J. J. Alwan, K. J. Beernink, J. S. Hughes and T.M. Cockerill, IEEE Photonics Technol. Lett. **3**, 6(1991).
10. R. D. Martin, S. Forouhar, S. Keo, R. J. Lang, R. G. Hunsperger, R. Tiberio, and P. F. Chapman, Electron. Lett. **30**, 1058 (1994)
11. R. D. Martin, S. Forouhar, S. Keo, R. J. Lang, R. G. Hunsperger, R. C. Tiberio, and P. F. Chapman, IEEE Photon. Technol. Lett. **7**, 244 (1995)